Carbapenems and SHV-1 β-Lactamase Form Different Acyl-Enzyme Populations in Crystals and Solution[†]

Matthew Kalp and Paul R. Carey*

Department of Biochemistry, Case Western Reserve University, 10900 Euclid Avenue, Cleveland, Ohio 44106

Received May 7, 2008; Revised Manuscript Received September 10, 2008

ABSTRACT: The reactions between single crystals of the SHV-1 β-lactamase enzyme and the carbapenems, meropenem, imipenem, and ertapenem, have been studied by Raman microscopy. Aided by quantum mechanical calculations, major populations of two acyl-enzyme species, a labile Δ^2-pyrroline and a more tightly bound Δ^1-pyrroline, have been identified for all three compounds. These isomers differ only in the position of the double bond about the carbapenem nucleus. This discovery is consonant with X-ray crystallographic findings that also identified two populations for meropenem bound in SHV-1: one with the acyl C═O group in the oxyanion hole and the second with the acyl group rotated 180° compared to its expected position [Nukaga, M., Bethel, C. R., Thomson, J. M., Hujer, A. M., Distler, A. M., Anderson, V. E., Knox, J. R., and Bonomo, R. A. (2008) *J. Am. Chem. Soc.* (in press)]. When crystals of the Δ^1- and Δ^2-containing acyl-enzymes were exposed to solutions with no carbapenem, rapid deacylation of the Δ^2 species was observed by kinetic Raman experiments. However, no change in the Δ^1 population was observed over 1 h, the effective lifetime of the crystal. These observations lead to the hypothesis that the stable Δ^1 species is due to the form seen by X-ray with the acyl carbonyl outside the oxyanion hole, while the Δ^2 species corresponds to the form with the carbonyl inside the oxyanion hole. Soak-in and soak-out Raman experiments also demonstrated that tautomeric exchange between the Δ^1 and Δ^2 forms does not occur on the crystalline enzyme. When meropenem or ertapenem was reacted with SHV-1 in solution, the Raman difference spectra demonstrated that only a major population corresponding to the Δ^1 acyl-enzyme could be detected. The 1003 cm^{-1} mode of the phenyl ring positioned on the C3 side chain of ertapenem acts as an effective internal Raman intensity standard, and the ratio of its intensity to that of the 1600 cm^{-1} feature of Δ^1 provides an estimate of the relative populations of Δ^1. In solution, I_{1600}/I_{1003} equals 2, and in the crystal, I_{1600}/I_{1003} equals 1. This is strong evidence that the Δ^1 and Δ^2 acyl-enzymes in the crystal are present in approximately equal amounts, in agreement with the X-ray data. However, in solution there are twice as many Δ^1 species per Phe group, and this represents approximately 100% of the active sites, which is consistent with the observed inhibition of the enzyme's activity.

Carbapenems are used as antibiotics of last resort because they possess a broad spectrum of antimicrobial activity. In the United States, carbapenems in clinical use include imipenem, meropenem, ertapenem, and doripenem, the latter a recently approved ultrabroad spectrum injectable antibiotic (Figure 1). These antibiotics elicit cell death by binding to penicillin-binding proteins (PBPs) and inhibiting cell wall biosynthesis. Additionally, they act as potent inhibitors of serine β-lactamases produced by bacterial cells with IC_{50} values ranging from 0.01 to 10 μM for most class A enzymes (*1*). Nonetheless, the emergence of carbapenemases belonging to class A (KPC, NMC-A, SME)[1] and class D (OXA-23, -40, -51) β-lactamases threatens their clinical utility (*2, 3*). In order to combat β-lactamase-mediated resistance, it is necessary to compare the mechanisms of inhibition for carbapenemase and noncarbapenemase enzymes, such as SHV- or TEM-type β-lactamases, to yield insights for future

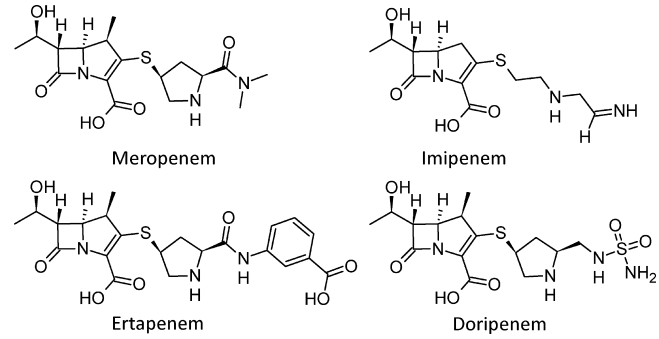

FIGURE 1: The carbapenems meropenem, ertapenem, imipenem, and doripenem are structurally similar to the penicillins, but the sulfur atom in position 4 is replaced by a carbon atom.

[†] Supported by NIH Grant RO1 GM54072 and the Case Western Reserve University MSTP Program.

* To whom correspondence should be addressed. E-mail: paul.carey@case.edu. Telephone: (216) 368-0031. Fax: (216) 368-3419.

[1] Abbreviations: TEM, class A β-lactamase of *Escherichia coli* first described in a Greek patient, with the acronym being derived from the patient's name, R, as in RTEM, indicates an inhibitor-resistant phenotype; SHV, class A β-lactamase of *Klebsiella pneumoniae* initially thought to be a "sulfhydryl variant" of the TEM enzyme; KPC, *K. pneumonia* carbapenemase; SME, class A β-lactamase from *Serratia marcescens* characterized by its significant activity against imipenem; NMC-A, nonmetallocarbapenamase of class A β-lactamases; OXA, oxacillinase group of β-lactamases (class D); HEPES, *N*-(2-hydroxyethyl)piperazine-*N*′-2-ethanesulfonic acid; HPLC, high-performance liquid chromatography.

10.1021/bi800833u CCC: $40.75
Published on Web 10/16/2008

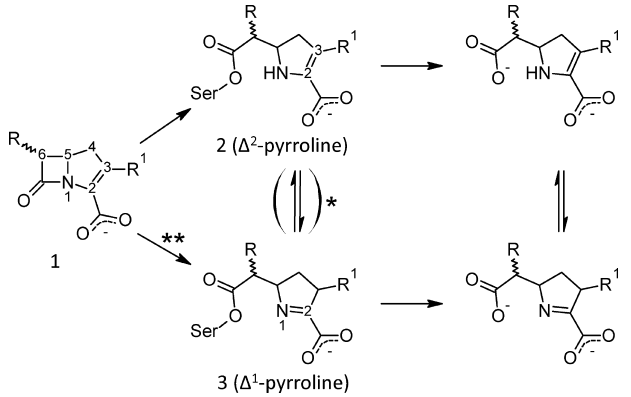

FIGURE 2: The proposed reaction scheme between a generalized carbapenem and SHV-1, a class A β-lactamase. Acylation of an active site residue, Ser70, results in partitioning of the carbapenem into either the Δ^1- or Δ^2-pyrroline. Unfavorable positioning of the Δ^1 acyl-enzyme in the SHV-1 active site results in a hydrolytically inert species. *Proposed by Zafaralla et al. but there is no evidence of a reversible step from our crystal data (*9*). **This mechanism is a proposal based on the present data.

drug design. To say that an acylation event between the carbapenem and β-lactamase leads to inhibition of the enzyme oversimplifies the inactivation chemistry; indeed, carbapenems, like clavulanate or the penam sulfones, sulbactam and tazobactam, undergo a secondary reaction inside the enzyme (*1, 4*). This mechanistic complexity provides an ideal opportunity to investigate the reactions between meropenem, ertapenem, and imipenem in single crystals of the class A β-lactamase SHV-1 by using a Raman microscope (*5, 6*). The resulting Raman difference spectroscopic data provide detailed information about the structures of various acyl-enzyme species along the reaction pathway as well as an estimate of their populations.

Charnas and Knowles first studied the kinetics of the interaction of RTEM β-lactamase with carbapenems and observed a biphasic hydrolysis profile with an initial burst phase that gave way to a slower steady-state reaction within a few minutes (*7, 8*). This hydrolysis profile was attributed to a kinetic scheme in which inhibition of the β-lactamase results from a branched reaction pathway (Figure 2). More specifically, attack of the catalytic serine on the β-lactam ring (species **1**) results in a newly formed acyl-enzyme species which can partition into either a Δ^2-pyrroline ester (species **2**) that undergoes rapid deacylation or a more hydrolytically inert Δ^1-pyrroline acyl-enzyme (species **3**). Later, Mobashery and co-workers suggested that, in class A enzymes, the guanidinium group of Arg244 or a water molecule coordinated to this moiety donates the proton required for the tautomerization of the Δ^2- to Δ^1-pyrroline ester (*9, 10*). Further implicating this residue in the tautomerization reaction, an inhibitor-resistant TEM with the Arg244Ser mutation showed monophasic hydrolysis of imipenem, due to displacement of this water molecule (*9*). In the class A β-lactamase used in the present study, SHV-1, replacement of Arg244 results in total loss of affinity for meropenem and decreased affinity for clavulanate (*11*). Together, these data imply that the same water molecule required for tautomerization in carbapenems also provides a critical proton for the formation of the inactivating species by clavulanic acid (*12*).

X-ray crystallographic studies with class A β-lactamases complexed with carbapenems reveal two important contributions to their efficacy as inhibitors. Initially, Knowles and colleagues postulated that imipenem and other carbapenems achieve inhibition by displacing *another* active site water (just adjacent to the nucleophilic serine) that participates in deacylation (*7, 8*). However, crystal structures with carbapenems covalently bound revealed that this deacylating water molecule is located in nearly the same position as in the apo structures, but a new hydrogen bond to the carbapenem's 6α-hydroxyethyl substituent weakens its nucleophilicity (*13*). Because this alone was unlikely to account for the efficacy of carbapenems against class A β-lactamases, it became clear some additional factor existed. The structure of SHV-1 with

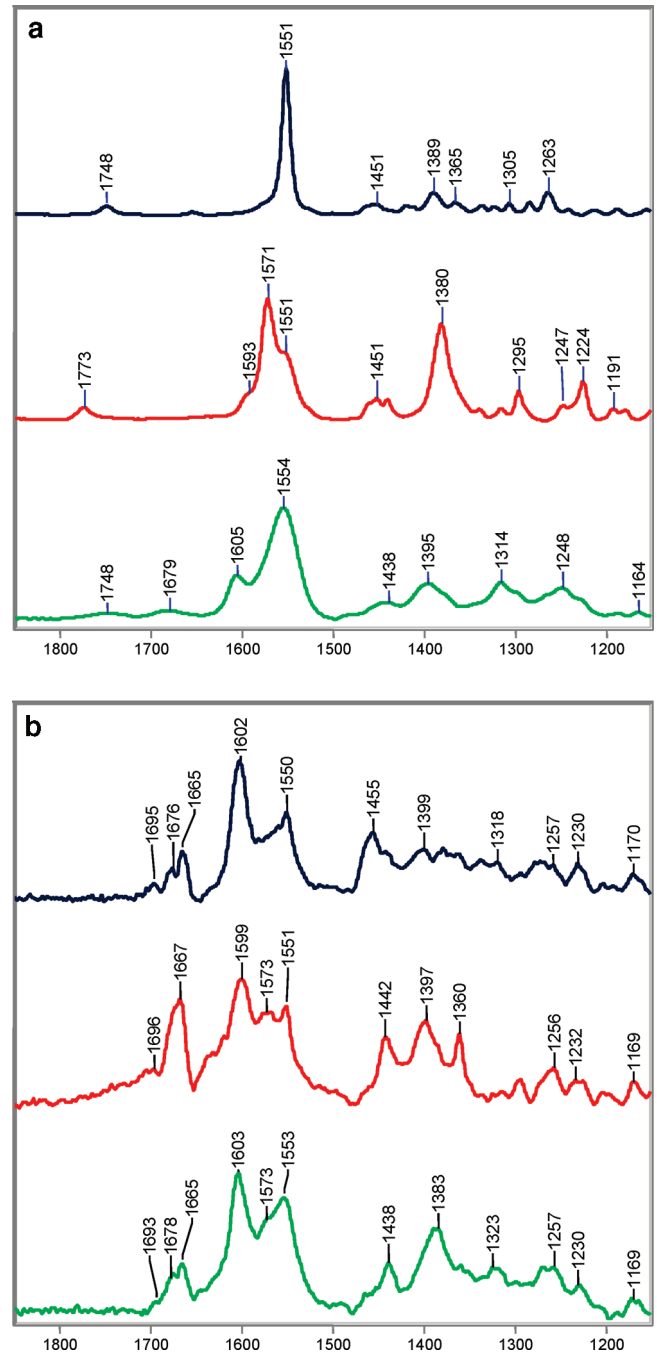

FIGURE 3: (a) Raman spectra of the unbound ligands meropenem (top), imipenem, and ertapenem (bottom). (b) Raman difference spectra of the meropenem (top), imipenem, and ertapenem (bottom) bound to SHV-1. The intense modes between 1550 and 1600 cm^{-1} provide detailed information arrangement of π-electrons in the carbapenem nucleus.

meropenem revealed that the carbonyl oxygen of the acyl group was "flipped outside" the oxyanion hole (*13*). However, this study did not attempt to relate the crystallographically observed species to the presence of the Δ^2- or Δ^1-pyrroline tautomers suggested by the original kinetic work (*13, 14*). Even at high resolution, hydrogen atoms are difficult to detect by X-ray diffraction; consequently, observation of the Δ^2- or Δ^1-pyrroline tautomers by X-ray analysis is problematic. Nonetheless, Raman difference spectra are very sensitive to the changes in peak frequencies that accompany this tautomerization (—CH═CH—NH— → —CH_2—CH═N—). Our investigation seeks to provide biophysical evidence for these tautomers and to describe their role in inhibiting the β-lactamase.

Raman crystallography has emerged as a unique tool in structural biology for investigating chemical reactions in single crystals (*5, 6*). Raman studies in conjunction with kinetic, structural, and mechanistic studies provide a heretofore missing link in the structural biology arsenal: notably, by relating the structural properties of the species detected by X-ray crystallography to those found in solution. In the present case, we see that mechanism-based inhibitors, such as carbapenems, behave very differently in the crystalline and solution phase of the SHV-1 β-lactamase.

EXPERIMENTAL PROCEDURES

Inhibitors. Clinical grade meropenem (Astra-Zeneca), ertapenem (Merck), and imipenem (Merck) were obtained from the Louis Stokes Veteran Affairs Medical Center pharmacy (Cleveland, OH) and were used without further purification. Stock solutions (20 mM) in 2 mM HEPES buffer (pH 7.0) were prepared for use with the protein crystals.

Protein Isolation and Purification. The SHV-1 β-lactamase enzyme was isolated and purified as previously described (*4*). An additional HPLC purification step was performed using a Sephadex Hi Load 26/60 column (Pharmacia, Uppsala, Sweden) and elution with phosphate-buffered saline (pH 7.4).

Crystallization. SHV-1 was concentrated to 5 mg/mL in 2 mM HEPES buffer (pH 7.0) for crystallization by the vapor diffusion method using the protocol of Kuzin et al. (*15*). Briefly, The 10 μL sitting protein drop [2 mg/mL, 0.56 mM Cymal-6 detergent (Hampton Research, Laguna Niguel, CA), 15% poly(ethylene glycol) 6000 (Hampton Research, Laguna Niguel, CA), 50 mM HEPES buffer, pH 7.0] was placed over a 0.50 mL reservoir solution containing 30% poly(ethylene glycol) and 100 mM HEPES buffer. The enzyme crystallized in approximately 1 week.

Raman Crystallography. The Raman microscope system has been described previously (*5, 6*). Using a cryoloop, crystals, typically 300 μm × 300 μm × 300 μm in size, were transferred from the mother liquor solution to a 4 μL drop of 2 mM HEPES. A 647 nm Kr^+ laser beam (Innova 70 C, Coherent, Palo Alto, CA) was focused on the protein crystals in a 4 μL hanging drop using the 20× objective of the Raman microscope. During data collection, spectra were acquired for 10 s, and 10 accumulations were averaged for each time point. After obtaining spectra of the apo β-lactamase protein crystals, inhibitors were added to the drop to achieve a final volume of 5 μL and a final inhibitor concentration of 5 mM. Spectra were then acquired every 2−3 min after addition of an inhibitor. To obtain difference spectra, an apo β-lactamase spectrum was subtracted from the protein:inhibitor spectra at varying time intervals following addition of inhibitor. For solution studies, 4 μL of a 940 μM solution of the β-lactamase in 2 mM HEPES, pH 7.0, was placed on a siliconized quartz coverslip and mounted in the hanging drop setup. Using the 20× objective of the Raman microscope, spectra of the apo β-lactamase were obtained, and subsequently, 1 μL of the inhibitor was added to achieve a final drop volume of 5 μL and a final inhibitor concentration of 750 μM. For the apo β-lactamases and enzyme/inhibitor complexes, 10 spectra were averaged with an acquisition of 60 s for each. Data collecting and processing were performed using HoloGRAMS and GRAMS/AI 7 software (ThermoGalactic, Inc., Salem, NH). Raman spectra of the inhibitors that were used were obtained under similar conditions. Spectra were obtained for 4 μL drops of inhibitor solutions prepared in 2 mM HEPES (pH 7.0) at varying inhibitor concentrations.

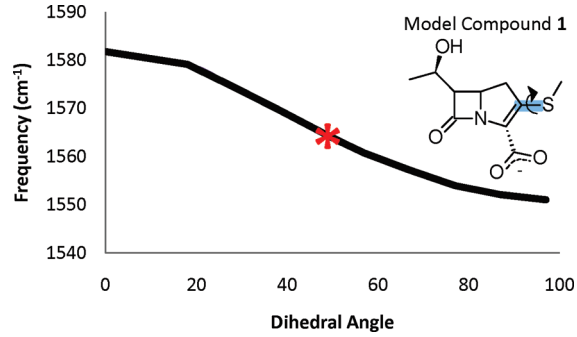

FIGURE 4: *Ab initio* calculations for molecule **1** (inset) demonstrate that the C2═C3 stretching frequency is sensitive to the C2═C3—S—C dihedral angle. While only the free ligand of imipenem exhibits rotational isomerism, complexation with the β-lactamase causes all of the carbapenems to adopt closely related rotational isomers for the Δ^2 acyl-enzyme *in crystallo*.

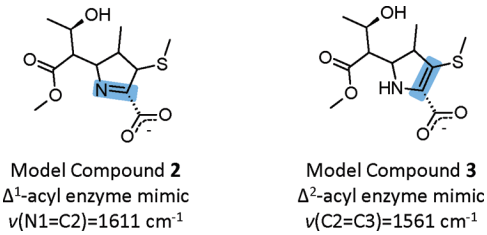

FIGURE 5: Structure of molecule **2**, Δ^1 acyl-enzyme mimic, and molecule **3**, Δ^2 acyl-enzyme mimic, with predicted stretching frequencies for the C═N and C═C stretches.

Synthesis of the Hydrolysis Products of Meropenem. Following the procedure of Easton and Knowles, an aqueous solution of meropenem (0.3 mM) and NaOH (0.6 mM) was incubated at 30 °C for 12 h, and the solution was then freeze-dried (*8*). The freeze-dried powder was resuspended under alkaline (pH 12) or neutral conditions (pH 7) in 50 mM sodium phosphate buffer, and Raman spectra were recorded immediately.

Calculations. Ab initio quantum mechanical calculations were performed to predict the Raman spectra of molecule **1** (see Figure 4) and molecules **2** and **3** (see Figure 5) using Gaussian 03 (*16*). Calculations were performed at the DFT level using the 6-31+G(d) basis set. DFT calculations were performed with Becke's three-parameter hybrid method using the correlation functional of Lee, Yang, and Parr (B3LYP), with 20% HF exact exchange mixing.

RESULTS AND DISCUSSION

Raman Spectra of Free Carbapenems. Figure 3a shows the Raman spectra of meropenem (top), imipenem, and ertapenem (bottom) in the 1150−1850 cm^{-1} region. The weak band near 1750−1775 cm^{-1} corresponds to the C═O stretch of the lactam carbonyl, a feature that is expected to shift to lower wavenumbers (1720−1740 cm^{-1}) upon ring opening and the acylation of the active site serine. Similarly, the carboxylate moiety at C2 is common to the carbapenems under investigation, and its symmetric stretch appears around 1400 cm^{-1}. Because each of the inhibitors shares the carbapenem nucleus and this includes a common delocalized π-electron system, this is expected to give rise to a similar intense feature in the Raman spectra. Thus, the dominant bands at 1550 cm^{-1} for meropenem and ertapenem and 1570 cm^{-1} for imipenem (with a significant shoulder at 1550 cm^{-1}) are assigned to a feature that has major contributions from the highly polarizable C2═C3 stretch, which is part of the π-electron system. Originally, we hypothesized that the 20 cm^{-1} difference is related to imipenem's lack of a C4 methyl group (see Figure 1), but *ab initio* calculations revealed that substitution at C4 does not significantly alter the C2═C3 stretch (Kalp and Carey, unpublished data). However, the calculations do provide support for the notion that imipenem exists as a mixture of rotational isomers about the C3−S bond, and this rotation impacts the C2═C3 stretching frequency. The results of a series of *ab initio* calculations on molecule **1** are shown in Figure 4. In this simulation, the frequency of the C2═C3 stretch was monitored as the C2═C3−S−C dihedral angle was rotated from its geometry-optimized position of 52°. The findings demonstrate that the C2═C3 stretching frequency can be significantly altered with limited rotation about the sulfide bond and that the observed 20 cm^{-1} difference in imipenem can be accounted for by an approximately 40° difference between the C2═C3−C−S dihedral angles of the two conformers. Namely, the 1570 and 1550 cm^{-1} bands observed in the solution spectrum of imipenem originate from rotational isomers with C2═C3−S−C dihedral angles of approximately 50° and 10°, respectively.

For imipenem, rotation about the C3−S bond is permitted due to the simplicity of its 2-(aminomethylideneamino)ethylsulfanyl side chain. This gives rise to a population of two energetically similar rotational isomers that can be observed by their distinct C2═C3 stretching frequencies. For meropenem and ertapenem, steric clashes between the bulky side chain and the carbapenem nucleus restrict rotation about the sulfide bond. As a result, only one isomer is detected by Raman spectroscopy in solution. Although, in the case of ertapenem, the broad peak centered at 1554 cm^{-1} suggests the presence of a number of closely lying conformational states making small excursions from the mean torsional angle, in all likelihood these states have similar energies and are rapidly interchanging. The spectroscopic study of the free ligands provides an essential basis for interpreting the 1550−1600 cm^{-1} double bond region of the acyl-enzyme complexes. However, the remaining regions of the spectra for meropenem, imipenem, and ertapenem are complex and consist of contributions that result from highly delocalized "coupled" vibrational modes. Since many of these change or disappear when the β-lactam ring opens upon acylation, they cannot be used as a basis for obtaining definitive information concerning enzyme−inhibitor interactions upon complexation.

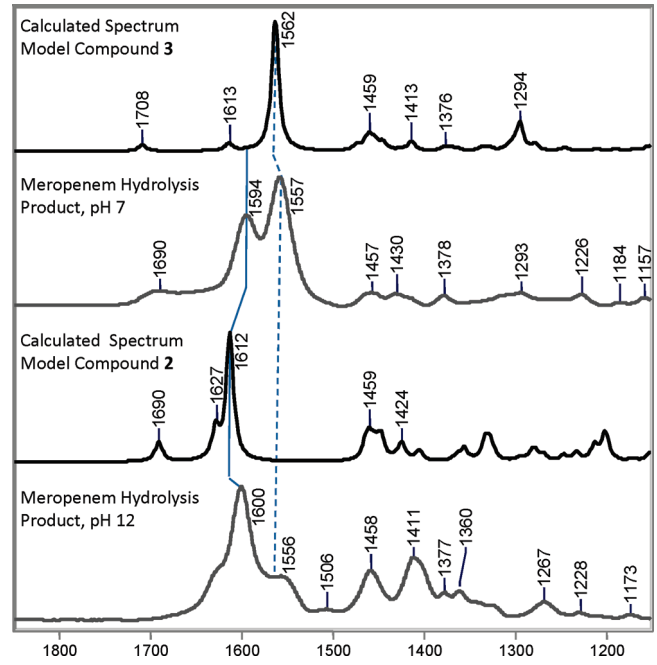

FIGURE 6: Predicted Raman spectra for molecules **2** and **3** (Figure 5), which mimic the Δ^1 or Δ^2 acyl-enzyme, respectively. The dominant features arise from the highly polarizable N1═C2 stretch around 1600 cm^{-1} (solid line) or C2═C3 stretching motions around 1550 cm^{-1} (dashed line). Hydrolysis of meropenem shows that the Δ^1-pyrroline is strongly favored thermodynamically over the Δ^2 isomer under basic conditions, while approximately equal amounts of the Δ^1 and Δ^2 isomers are present under acidic conditions.

Carbapenems Form Two Distinct Acyl-Enzyme Populations in SHV-1 Crystals. As the inhibitors soak into the β-lactamase crystals, they react in the active site and proceed on the reaction pathway outlined in Figure 2. The Raman difference spectra of meropenem (top), imipenem, and ertapenem (bottom) after they diffuse into the crystal for ~20 min are shown in Figure 3b. Although these difference spectra bear little resemblance to those of the free inhibitors, the major features can be assigned. The major contributions to the difference spectra are from the bound ligand, but peaks due to protein modes are also present since a protein conformational change occurs upon ligand binding. The major features in Figure 3b, between 1550 and 1600 cm^{-1}, are associated with double bond stretching motions. Detailed assignments can be made based on quantum mechanical calculations on molecules **2** and **3** (Figure 5), which are models for the pyrroline tautomers shown in Figure 2. The methyl ester was chosen to mimic the serine acyl-enzyme while the complex thioether moiety was truncated to a methyl group. The calculated spectra for **2** and **3** are shown in Figure 6. The figure also shows spectra of the nonenzymatic hydrolysis products of meropenem resuspended under basic and neutral conditions. Base-catalyzed hydrolysis of the β-lactam gives a nonequilibrium ratio of C-3 epimers of the Δ^1 tautomer (Figure 2). When the product of base hydrolysis is resuspended, the Δ^1- → Δ^2-pyrroline tautomerization is rapid near neutrality but relatively slow at high pH, and Raman spectra of the nonenzymatic hydrolysis products immediately after resuspension support this finding (*8*). As seen in Figure 6, the hydrolysis product rapidly equilibrates

under neutral conditions to form an equal mixture of Δ^1 and Δ^2 tautomers as evidenced by similar Raman intensities at 1594 cm^{-1} and 1574 cm^{-1} whereas the Δ^1-pyrroline is predominant over the Δ^2 isomer at higher pH.

The calculations and nonenzymatic hydrolysis species immediately suggest that the acyl-enzyme band near 1600 cm^{-1} in Figure 3b is due to the N1═C2 stretch of the Δ^1-pyrroline tautomer while the acyl-enzyme band near 1550 cm^{-1} is due to the Δ^2-pyrroline tautomer. Because the N1═C2 of molecule **2** and C2═C3 of molecule **3** (Figure 5) occur in a five-membered ring, their stretching frequencies are decreased compared to the typical group stretching frequencies of imines and alkenes. Taken together, these data provide the first biophysical evidence that two major tautomer populations, the Δ^1- and Δ^2-pyrroline tautomers, are formed in the reaction between carbapenems and SHV-1. These correspond to the two conformations detailed in the X-ray crystallographic analysis. Although the spectra seen in Figure 3b are shown at 20 min, they are invariant over 5−60 min showing that the populations do not "funnel-down" into a single, more thermodynamically stable form. This is illustrated graphically by plotting the peak height ratios I_{1600}/I_{1550} as a function of time in Supporting Information Figure S1.

Adding another layer of complexity, spectral evidence indicates that one of these major populations, the Δ^2 tautomer, is composed of at least two minor components. In the previous section, we demonstrated that, in solution, imipenem exists as a pair of rotational isomers about the C3—S bond, with the isomer that gives rise to the 1570 cm^{-1} band predominating. Now, complexation with the β-lactamase results in a redistribution of these rotational isomers so that neither conformation is favored in the active site. This is evidenced by nearly equal intensity contributions in the 1575−1550 cm^{-1} regions for acyl-enzyme (Figure 3b). While steric hindrance disallowed rotation about the C3—S for meropenem and ertapenem in solution, their difference spectra in the crystal complex show unresolved intensity between the 1600 and 1550 cm^{-1} regions, suggesting that, like imipenem, a population of rotamers also exists giving rise to Raman bands near 1570 cm^{-1}. Thus, binding of each inhibitor to the β-lactamase results in the C3 side chain assuming at least two conformations. For meropenem, the flexibility of this side chain is reiterated by Nukaga et al., where multiple weak electron density features beyond its sulfide linkage prevent definitive modeling in the binding cleft (*14*). Although no crystallographic evidence is available for the acyl-enzymes formed between SHV-1 and imipenem or ertapenem, spectral similarities to meropenem suggest that, once bound, flexibility of the C3 side chain is universal. While there is a paucity of structural information regarding the complexes formed between carbapenems and serine β-lactamases, there are reports that the side chains of meropenem and imipenem adopt two different conformations with the class D β-lactamase OXA-13 (*17*). In one conformation, the long sulfur-containing side chain protrudes outside of active site whereas the side chain of the other conformer lies against the loop connecting strand β9 to helix α9, near Glu244. In addition, we have not been able to detect with confidence the expected acyl-enzyme C═O stretch in the 1720−1740 cm^{-1} region. It is likely a weak, broad band that is not seen at the present level of signal to noise.

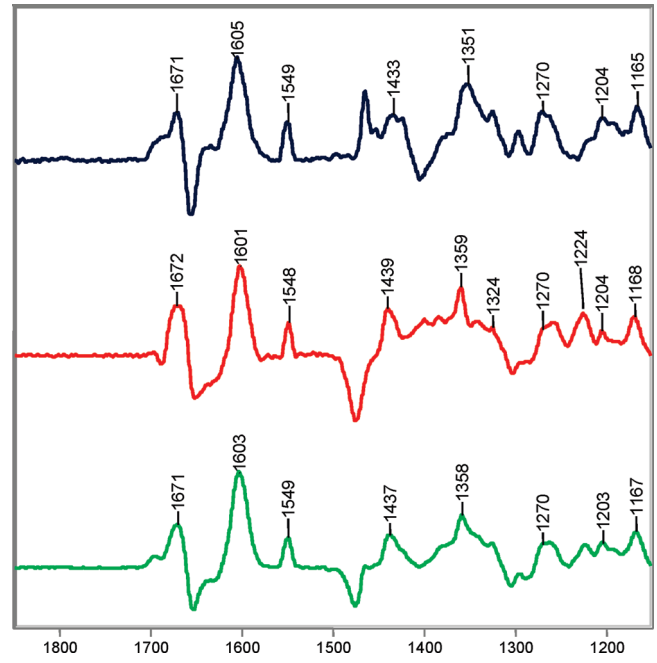

FIGURE 7: Raman difference spectra of a "soak-out" experiment for meropenem (top), imipenem, and ertapenem (bottom). The dominant band at 1600 cm^{-1} indicates that the Δ^1 tautomer does not deacylate from the enzyme. Features associated with protein modes, such as 1670 and 1324 cm^{-1}, indicate a "tightening" of the β-sheet motifs upon complexation.

Most of the other features observed in Figure 3b are due to protein modes caused by ligand-induced conformational change. An exception is the broad peak near 1390 cm^{-1} that is assigned to a mode with major contribution from the symmetric stretch of the ligand's —COO^- group at position 2. The peaks near 1667 cm^{-1} are assigned to amide I vibrations from the β-sheet. It is envisaged that ligand binding causes a small increase in the secondary structure or a tightening of an existing β-sheet that augments its effective Raman intensity. Normalizing the 1667 cm^{-1} band intensity to the amide I band intensity in the apo spectrum predicts that the intensity change is equivalent to only ~5% of the residues experiencing this perturbation of secondary structure. Similarly, the minor peaks near 1230 cm^{-1} are assigned to β-sheet amide III modes, while the peaks near 1255 cm^{-1} are tentatively ascribed to amide III vibrations from peptide bonds not in regular secondary structure. The features in the 1440−1445 cm^{-1} region are probably due to C—H motions such as —CH_2— deformations originating in the inhibitor or the protein. The conformational change is discussed further in the next section.

In Crystals the Δ^1 Acyl-Enzyme of Carbapenems Is Stable and the Δ^2 Form Deacylates Rapidly. Because carbapenems partition into conformationally and chemically distinct molecules in the β-lactamase's active site, desoaking experiments were performed to characterize the relative lability of the bound forms. A protein crystal was soaked in a 5 mM bath of meropenem, imipenem, or ertapenem for 20 min and then transferred to a buffer solution in the absence of ligand. The resulting Raman difference spectra, [carbapenem-treated crystal] − [apo crystal], after transfer are shown in Figure 7, where only features due to the Δ^1 tautomer remain. Although shown in Figure 7 at 5 min, the intensity of the 1600 cm^{-1} band is constant for the lifetime of the crystal,

or approximately 1 h, suggesting that the Δ^1 tautomer forms a long-lived and irreversible acyl-enzyme. Quantitative data are given in Supporting Information Figure S2. The results of these "soak-out" experiments imply that Δ^1 to Δ^2 tautomerization does not occur on the enzyme. This finding echoes the outcome of timed mass spectrometry experiments by Nukaga et al., who demonstrated that, with SHV-1, the meropenem acyl-enzyme persists for at least 1 h in solution (*14*). Compared to the difference spectra under steady-state conditions in Figure 3b, the Raman data in Figure 7 reveal that a reactive species, the Δ^2 acyl-enzyme at 1550−1570 cm^{-1}, deacylates within the time resolution of our experiment of a few minutes.

In a high-resolution crystal structure of the SHV-1−meropenem complex, two serine-bound intermediates are present with approximately equivalent occupancies (*14*). In one conformation, the carbonyl oxygen of the acyl group is "flipped" *outside* the oxyanion hole by approximately 180°, a position that deactivates it to hydrolytic attack. In the second conformation, the carbonyl oxygen is located *inside* the oxyanion hole with the amide backbone of residues Ser70 and Ala237 hydrogen bonded with the acyl C═O group. While the X-ray structure detects two conformations of meropenem in the active site, it can neither differentiate between the Δ^1- and Δ^2-pyrroline tautomers nor assess the reactivity of the two conformers. However, Raman crystallography provides characteristic signatures for the Δ^1 and Δ^2 tautomers and allows these populations to be monitored. Thus, this synergistic approach allows us to predict that the species *inside* the oxyanion hole, as described by X-ray crystallographic studies, is the reactive Δ^2 tautomer that undergoes deacylation upon desoaking. Correspondingly, the species observed *outside* the oxyanion hole is the hydrolytically inert Δ^1 conformer that remains bound to Ser70 for at least 1 h.

The relationship between the Δ^1 and Δ^2 tautomers is complex and is only partially understood. The experimental results are as follows:

(1) We detect Δ^1 and Δ^2 species bound in the crystals under steady-state soak-in conditions using Raman microscopy. We assign these to the two populations characterized by X-ray crystallography. The ratio of Raman intensities of the two species is invariant with time (Figure 3b and Supporting Information Figure S1).

(2) Upon soaking out in buffer, the Raman signature of Δ^2 disappears, which leaves an invariant signature due to the Δ^1 species (Figure 7 and Supporting Information Figure S2).

(3) In Figure 7, there is evidence for protein conformational change. This includes the amide I β-signature near 1670 cm^{-1} and tryptophan modes near 1550, 1350, and 1000 cm^{-1} (the latter not shown). The protein modes vary according to the ligand but are very similar between steady-state conditions (Figure 3b) and soak-out in buffer (Figure 7).

(4) Only the Δ^1 species is detected in solution, and there is no evidence for protein peaks due to conformational changes in solution (see next section and Figure 8).

The time invariance of Figure 7 shows that $\Delta^1 \rightarrow \Delta^2$ interconversion does not occur within the crystals. Moreover, the time invariance of Figure 3 shows that the "Δ^2 active sites" do not empty to be gradually replaced by Δ^1 species.

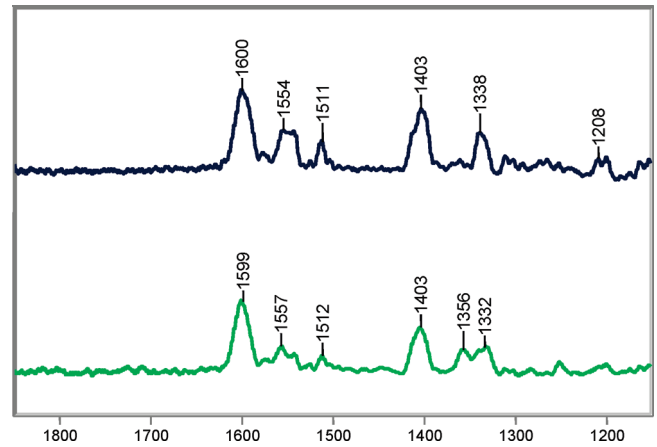

FIGURE 8: Solution Raman difference spectra of meropenem (top) and ertapenem (bottom) bound to SHV-1 in 1:1 complex at 750 μM in 2 mM HEPES at pH 7.0.

This may be associated with the subtle protein conformational change we have detected in the crystal, and these may be trapped by crystal packing forces. There are no major changes detected by X-ray analysis; thus, the spectroscopic changes we detect could be due to a damping of protein motion caused by ligand binding. Another possibility is that we are seeing tight binding of product in the Δ^2 sites, which prohibits reacylation by fresh substrate. In this regard, hydrolysis product inhibition has also been observed for carbapenems with TEM β-lactamases (*10*).

In Solution SHV-1 and Carbapenems Form a Single, Inactive Acyl-Enzyme. If, in contrast to the crystal behavior, conformational cycling of the β-lactamase is permitted in solution, then the reaction between SHV-1 and meropenem, imipenem, or ertapenem should predominantly, if not exclusively, result in a population of Δ^1 acyl-enzymes. Following inhibitor reactions in solution by Raman spectroscopy demands high protein concentrations (approximately 750 μM or 25 mg/mL) and stoichiometric amounts of ligand. Although the concentrations attainable result in a low S/N ratio, difference spectra could be obtained for meropenem and ertapenem with SHV-1 (Figure 8). For both ligands, a key acyl-enzyme band near 1600 cm^{-1} denotes the presence of a large population of Δ^1 acyl-enzymes. This band is accompanied by the symmetric stretch of the carboxylate near 1400 cm^{-1}, which makes significant contributions to the difference spectra. Unlike the poorly defined carboxylate stretches observed in the crystal phase for meropenem and ertapenem, the Raman band shape in the solution phase suggests a homogeneous environment is experienced by the $-CO_2^-$ group; i.e., a dominant population of the Δ^1 tautomer is present. Of note, the numerous protein modes that contribute to the difference spectra in the crystal phase are not observed in solution; this further supports the hypothesis that interconversion between conformational states is rapid in solution but prohibited in the crystal and that, due to protein−protein contacts, conformational changes become "trapped" in the crystal phase. The Raman data seen in Figure 8 are recorded on the time scale of minutes. We cannot distinguish between the possibilities that Δ^1 is exclusively formed under stoichiometric conditions or the Δ^2 species is formed but quickly transforms to Δ^1 in the experimental dead time.

For ertapenem, a narrow 1003 cm^{-1} feature arises from the aromatic moiety of the C3 side chain and provides an

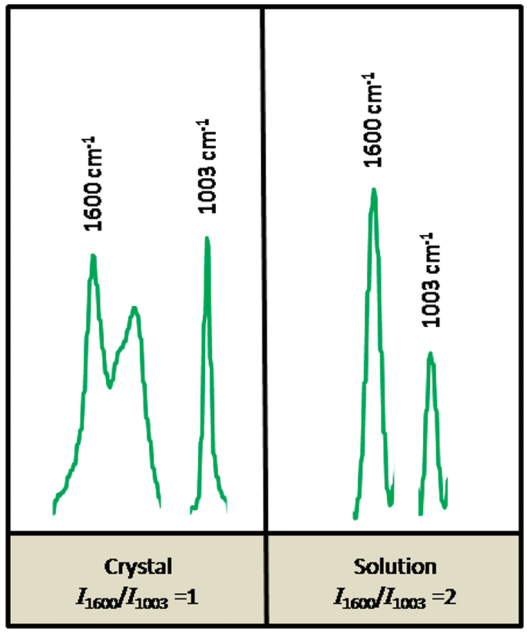

FIGURE 9: Partial Raman difference spectra for ertapenem in crystal and solution. The 1003 cm^{-1} mode of the phenyl ring positioned on the C3 side chain of ertapenem acts as an effective internal intensity standard, and the ratio of its intensity (I) to that of the 1600 cm^{-1} feature of Δ^1 provides an estimate of the relative populations of Δ^1. In solution, I_{1600}/I_{1003} equals 2, whereas I_{1600}/I_{1003} equals 1 in the crystal.

important means of quantifying the relative amounts of the Δ^1 acyl-enzyme formed in the crystal and solution phases. Because the phenyl group is common to both tautomers, its intensity is proportional to the total amount of ertapenem acyl-enzyme formed in either phase, assuming no enzyme contribution and no orientation dependence to the 1003 cm^{-1} mode. Thus, normalizing the 1600 cm^{-1} band relative to the 1003 cm^{-1} band allows us to estimate the amount of Δ^1 acyl-enzyme in the crystal or solution phases. In the crystal, the I_{1600}/I_{1003} ratio is approximately 1. In contrast, the I_{1600}/I_{1003} ratio is approximately 2 in solution (Figure 9). These results demonstrate that the relative population of Δ^1 in solution is double that found in the crystal. They also suggest that approximately equal amounts of the Δ^1 and Δ^2 are formed in the crystal. In both the meropenem and ertapenem difference spectra, the intensity observed near 1550−1530 cm^{-1} probably results from a composite of a small amount of ligand, turnover product, and subtraction difficulties inherent to Raman spectroscopy in solution, although the presence of a minor population of the Δ^2 species cannot be ruled out.

In conclusion, we show that the results of X-ray crystallography experiments between inhibitors, such as carbapenems, and β-lactamases must be interpreted with caution as different intermediates and populations may exist in the crystal and solution phases. This duality affects rational drug design which seeks to exploit complementarity between the ligand and the active site. For carbapenems and SHV-1, both Raman and X-ray crystallography detect two conformers in the active site: the Δ^1 acyl-enzyme is a long-lived, hydrolytically inert species, while the Δ^2 acyl-enzyme rapidly deacylates when challenged by a soak-out experiment. The most substantive chemical difference between the Δ^1 and Δ^2 tautomers is the presence of the —NH— group in Δ^2. Thus, it is possible to speculate that the presence or absence of the —NH— group can trigger the modest protein conformational change observed. This idea has been put forward in earlier work by Faraci and Pratt while studying the mechanism of inhibition of the PC1 β-lactamase of *Staphylococcus aureus* by cephalosporins (*18*). Moreover, the inert nature of the Δ^1 species derives not only from possible conformational changes at the enzyme active site but also from subtle differences in ligand positioning, especially with respect to the acyl group. Greater enzyme plasticity in solution as compared to the crystal phase may prevent detection of protein conformational change by Raman spectroscopy; however, we unambiguously identify the Δ^1 tautomer as the primary inhibitory species. With both "inhibitor" and "substrate" binding modes present in the crystal, our results emphasize that caution has to be exercised when translating X-ray results to define inhibition in solution or *in vivo*.

ACKNOWLEDGMENT

We thank David Ahn and Marianne P. Carey for assistance with protein production, purification, and crystallization and Robert A. Bonomo for the generous gift of the SHV-1 clone.

SUPPORTING INFORMATION AVAILABLE

Time dependence of the peak intensity ratio of the 1600 cm^{-1} band to the 1550 cm^{-1} band (Figure 1) and time dependence of the peak intensity ratio of the 1600 cm^{-1} band to amide I (Figure 2). This material is available free of charge via the Internet at http://pubs.acs.org.

REFERENCES

1. Page, M. G. (2000) β-Lactamase inhibitors. *Drug Resist. Updates 3*, 109–125.
2. Ke, W., Bethel, C. R., Thomson, J. M., Bonomo, R. A., and van den Akker, F. (2007) Crystal structure of KPC-2: insights into carbapenemase activity in class A β-lactamases. *Biochemistry 46*, 5732–5740.
3. Brown, S., and Amyes, S. (2006) OXA (beta)-lactamases in Acinetobacter: the story so far. *J. Antimicrob. Chemother. 57*, 1–3.
4. Totir, M. A., Padayatti, P. S., Helfand, M. S., Carey, M. P., Bonomo, R. A., Carey, P. R., and van den Akker, F. (2006) Effect of the inhibitor-resistant M69V substitution on the structures and populations of *trans*-enamine β-lactamase intermediates. *Biochemistry 45*, 11895–11904.
5. Carey, P. R. (2006) Raman crystallography and other biochemical applications of Raman microscopy. *Annu. Rev. Phys. Chem. 57*, 527–554.
6. Carey, P. R. (2006) Spectroscopic characterization of distortion in enzyme complexes. *Chem. Rev. 106*, 3043–3054.
7. Charnas, R. L., and Knowles, J. R. (1981) Inhibition of the RTEM β-lactamase from Escherichia coli—Interaction of enzyme with derivatives of olivanic acid. *Biochemistry 20*, 2732–2737.
8. Easton, C. J., and Knowles, J. R. (1982) Inhibition of the RTEM β-lactamase from Escherichia coli—Interaction of the enzyme with derivatives of olivanic acid. *Biochemistry 21*, 2857–2862.
9. Zafaralla, G., and Mobashery, S. (1992) Facilitation of the Δ^2 to Δ^1 pyrroline tautomerization of carbapenem antibiotics by the highly conserved arginine-244 of class A β-lactamases during the course of turnover. *J. Am. Chem. Soc. 114*, 1505–1506.
10. Taibi, P., and Mobashery, S. (1995) Mechanism of turnover of imipenem by the TEM β-lactamase revisited. *J. Am. Chem. Soc. 117*, 7600–7605.
11. Thomson, J. M., Distler, A. M., Prati, F., and Bonomo, R. A. (2006) Probing active site chemistry in SHV β-lactamase variants at Ambler position 244. Understanding unique properties of inhibitor resistance. *J. Biol. Chem. 281*, 26734–26744.

12. Imtiaz, U., Billings, E., Knox, J. R., Manavathu, E. K., Lerner, S. A., and Mobashery, S. (1993) Inactivation of class A β-lactamases by clavulanic acid—The role of arginine-244 in a proposed nonconcerted sequence of events. *J. Am. Chem. Soc. 115*, 4435–4442.
13. Maveyraud, L., Mourey, L., Kotra, L. P., Pedelacq, J. D., Guillet, V., Mobashery, S., and Samama, J. P. (1998) Structural basis for clinical longevity of carbapenem antibiotics in the face of challenge by the common class A β-lactamases from the antibiotic-resistant bacteria. *J. Am. Chem. Soc. 120*, 9748–9752.
14. Nukaga, M., Bethel, C. R., Thomson, J. M., Hujer, A. M., Distler, A. M., Anderson, V. E., Knox, J. R., and Bonomo, R. A. (2008) Inhibition of class A β-lactamases by carbapenems: Crystallographic observation of two conformations of meropenem in SHV-1. *J. Am. Chem. Soc.* (in press).
15. Kuzin, A. P., Nukaga, M., Nukaga, Y., Hujer, A. M., Bonomo, R. A., and Knox, J. R. (1999) Structure of the SHV-1 β-lactamase. *Biochemistry 38*, 5720–5727.
16. Frisch, A., Frisch, M. J., and Trucks, G. W. (2003)Gaussian, Inc., Wallingford, CT.
17. Pernot, L., Frenois, F., Rybkine, T., L'Hermite, G., Petrella, S., Delettre, J., Jarlier, V., Collatz, E., and Sougakoff, W. (2001) Crystal structures of the class D β-lactamase OXA-13 in the native form and in complex with meropenem. *J. Mol. Biol. 310*, 859–874.
18. Faraci, W. S., and Pratt, R. F. (1985) Mechanism of inhibition of the PC1 β-lactamase of Staphylococcus aureus by cephalosporins: Importance of the 3′-leaving group. *Biochemistry 24*, 903–910.

BI800833U